European Journal of Mechanics / B Fluids 111 (2025) 308–318

Contents lists available at ScienceDirect

European Journal of Mechanics / B Fluids

journal homepage: www.elsevier.com/locate/ejmflu

Sensitivity analysis for incompressible Navier–Stokes equations with uncertain viscosity using polynomial chaos method

N. Nouaime [a,b,*], B. Després [b], M.A. Puscas [a], C. Fiorini [c]

[a] Université Paris-Saclay, CEA, DES, ISAS, Modeling of Structure and Systems Department, Center of Saclay, 91191, Gif-sur-Yvette Cedex, France
[b] Sorbonne Université, CNRS, Université de Paris, Laboratoire Jacques-Louis Lions (LJLL), F-75005, Paris, France
[c] M2N, Conservatoire National des Arts et Métiers, Paris, France

ARTICLE INFO

Keywords:
Navier–Stokes equations
Polynomial chaos method
Finite element-volume scheme

ABSTRACT

We present a stability estimate for the sensitivity of the incompressible Navier–Stokes equations under uncertainty in model parameters such as viscosity and initial or boundary conditions. The approach employs the stochastic Galerkin method, wherein the solution is represented using a generalized polynomial chaos expansion. The governing equations are projected onto stochastic basis functions, resulting in an extended coupled equation system. These coupled equations are challenging to solve numerically. A decoupling method is proposed to simplify their numerical resolution, which, along with the stability estimates, represents one of this study's most valuable and original aspects. Finally, we present the lid-driven cavity numerical test to evaluate the polynomial chaos method and compare the solutions with the numerical data published in the literature.

1. Introduction

In fluid dynamics, the Navier–Stokes equations describe the fundamental principles governing the dynamics of viscous fluid flows. Despite their deterministic nature, real-world fluid systems naturally contain uncertainties from various sources, such as uncertain boundary conditions, initial conditions, and input parameters. These uncertainties pose significant challenges to accurately predict and understand fluid behavior using traditional deterministic models. Sensitivity analysis is a possible strategy for quantifying the sensitivity of fluid flow simulations to uncertainties. In this paper, we adapt this approach to the Navier–Stokes equations, using the Polynomial Chaos Method (PCM).

Over the years, the PCM has become a widely used technique for uncertainty quantification and sensitivity analysis. Its evolution has been characterized by a growing recognition of its fundamental role in resolving the complex interaction between uncertain input parameters and model outputs. The PCM has been extensively applied in various fields, including heat transfer problems [1,2], thermal-hydraulics [3,4] and porous media [5–7]. It is also applied to solid mechanics problems, which often involve complex nature and multiple interacting physical phenomena [8]. Furthermore, it is used in fluid–structure interactions [9–12], in which the interactions between one or more structures and fluid flows present significant challenges due to their nonlinear and multidisciplinary nature. Additionally, the PCM finds application in various other fields, including chemical processes [13] and radioactive decay [14]. This work focuses on using the PCM in Computational Fluid Dynamics (CFD), and particularly on its application to the Navier–Stokes equations. In Polynomial Chaos Expansion (PCE), random variables are expressed as linear combinations of orthogonal polynomials, with the coefficients representing the contributions of each polynomial basis function to the expansion. The PCM was first introduced in [15] in 1938 with Wiener's theory of homogeneous chaos. In 2002, Xiu and Karniadakis [16] extended polynomial chaos to generalized polynomial chaos (gPC) for the polynomials of the Askey scheme. Later, this method was further extended to arbitrary distributions in [17]. In this approach, the random variables are expressed as linear combinations of orthogonal polynomials called Polynomial Chaos Expansion (PCE). The main goal of the PCM is to compute the coefficients of the linear combinations in the PCE since they capture the influence of the uncertainties in the input variables on the solution. This can be achieved through either an intrusive approach [18,19], in which the governing equations are projected onto the subspace spanned by the PC basis using the Galerkin formulation, or non-intrusive approach [12,20], in which the existing deterministic solvers are treated as a black box. Both approaches have their advantages, and the

* Corresponding author at: Université Paris-Saclay, CEA, DES, ISAS, Modeling of Structure and Systems Department, Center of Saclay, 91191, Gif-sur-Yvette Cedex, France.
E-mail addresses: nathalie.nouaime@cea.fr (N. Nouaime), bruno.despres@sorbonne-universite.fr (B. Després), maria-adela.puscas@cea.fr (M.A. Puscas), camilla.fiorini@lecnam.net (C. Fiorini).

https://doi.org/10.1016/j.euromechflu.2025.01.012
Received 7 June 2024; Received in revised form 20 January 2025; Accepted 27 January 2025
Available online 7 February 2025

choice between them depends on the problem's particular demands, the model's complexity, and the available resources. The non-intrusive approach is easy to implement and can be used with black-box models where the equations are not explicitly available. On the other hand, the intrusive approach proves to be more efficient when code modification is feasible and very efficient in terms of numerical computation time. This work considers the Intrusive Polynomial Chaos Method (IPCM). The IPCM method recently became a very used and efficient method for uncertainty quantification [21], efficient in terms of computational time [22] especially when applied to complex models like the Navier–Stokes equations.

Specifically, we are interested in the efficient computation of solutions of the Navier–Stokes equations with uncertain viscosity and uncertain initial or boundary conditions [19]. Uncertain viscosity is a significant problem in many domains. Such as biomedical flows, more precisely the blood flow viscosity problem, where the blood viscosity uncertainty is investigated and its effect on the quantities of interest, such as wall shear, pressure and mass flow split [23,24], is quantified. The uncertain viscosity problem is critical in engineering applications such as aeroelasticity [25], nuclear industry [26,27], turbomachinery [28], energy harvesting of flexible structures [29], etc.

In the following, we use the intrusive PCM to compute the first-order sensitivity of the Navier–Stokes equations. We prove the well-posedness of the sensitivity equations, i.e., that they have a unique solution that is continuously dependent on the input data, using an energy estimate inspired by the proof detailed in [30]. Firstly, we consider only one uncertain parameter within the Navier–Stokes equations. Secondly, we extend this approach to incorporate the multivariate polynomial chaos method to handle scenarios where more than one parameter is uncertain. Two types of multivariate polynomial chaos methods exist: one involves independent random variables, while the other involves dependent random variables.

The PCM for multivariate independent random variables is considered and extended from the univariate PCM, where the orthogonal multivariate polynomials are the product of the constructed univariate orthogonal polynomials [31]. The PCM for multivariate dependent variables is described in many papers [31,32], where they present approaches to construct a basis of the probability space of orthogonal polynomials for general multivariate distributions with correlations between the random input variables. A goal of our work is, among other things, to calculate the variance of the solution of the Navier–Stokes equations when there are uncertain parameters. This is called Uncertainty Quantification (UQ). There are many approaches to do this, but in this paper the PCM is used and then compared to the Taylor expansion and the result is extremely accurate.

The original contributions of this work are the following:

(i) We show a stability estimate for the Navier–Stokes solution and its sensitivity.
(ii) We present an approach that involves decoupling the coupled equations resulting from applying the intrusive PCM to the Navier–Stokes equations. This decoupling method makes it possible to separate the equations, which is highly convenient for implementation in a pre-existing code.
(iii) Finally, we will present numerical result for the lid-driven cavity problem, with an uncertain viscosity, with uncertain boundary condition and, finally, with both uncertainties. We present an estimate of the mean and the standard deviation of the uncertain variables.

This paper is structured as follows. In Section 2 the physical model is presented. In Section 3 the univariate polynomial chaos method is introduced as well as the multivariate PCM and its significance in computing the mean and variance of the uncertain variable using the expansion coefficients directly, when more than one parameter is uncertain. In Section 4, the PCM is applied to the Navier–Stokes equations, and the well-posedness of the sensitivity equations is discussed. In Section 5 an approach that involves decoupling for the coupled equations resulting from applying the intrusive PCM to the Navier–Stokes equations, is introduced. In Section 6 the well-known lid-driven cavity numerical test is presented, in which three scenarios are presented: one involving uncertain fluid viscosity, one involving uncertain boundary conditions (specifically the lid-driven velocity), and one involving uncertainties in both parameters.

2. Physical model

Let $\Omega \in \mathbb{R}^2$ be a domain that has a Lipschitz-continuous boundary. The incompressible Navier–Stokes equations [33,34] consist in finding $(\mathbf{u}, p)$ such that:

$$\begin{cases} \partial_t \mathbf{u}(\mathbf{x},t) - \nu \Delta \mathbf{u}(\mathbf{x},t) + (\mathbf{u}(\mathbf{x},t)\cdot\nabla)\mathbf{u}(\mathbf{x},t) + \nabla p(\mathbf{x},t) = \mathbf{f}(\mathbf{x}) & \Omega,\ t>0, \quad (1a)\\ \nabla\cdot\mathbf{u}(\mathbf{x},t) = \mathbf{0} & \Omega,\ t>0, \quad (1b)\\ \mathbf{u}(\mathbf{x},0) = \mathbf{0} & \Omega,\ t=0, \quad (1c)\\ \mathbf{u}(\mathbf{x},t) = \mathbf{g}(\mathbf{x},t) & \Gamma=\partial\Omega,\ t>0. \quad (1d) \end{cases}$$

where $\mathbf{u}(\mathbf{x},t) = (u(\mathbf{x},t), v(\mathbf{x},t))$ is the velocity, p is the pressure, $\mathbf{f} = (f^x, f^y)$ is the stationary external force and $\mathbf{g}(\mathbf{x},t) = (g^x(\mathbf{x},t), g^y(\mathbf{x},t))$ the Dirichlet boundary condition. The first equation models the conservation of the momentum and the second one the conservation of the mass. For the sake of simplicity, only homogeneous Dirichlet boundary conditions are considered. We consider that the conditions such that there exists a unique variational solution $(\mathbf{u}, p) \in H_0^1(\Omega)^2 \times L_0^2(\Omega)$ are met [33,34].

3. Overview of the PCM

The intrusive PCM consists of replacing the uncertain variables in the Navier–Stokes equations with their PCE to model uncertainty propagation. The resulting equations are projected onto orthogonal polynomials, yielding deterministic equations. This process provides a compact representation of the output variable with respect to the inputs, creating the sensitivity model. This section introduces the univariate PCM as well as the multivariate method.

3.1. The univariate PCM

We consider the case where the viscosity ν or the initial or boundary conditions are uncertain. The variables $\mathbf{u}$ and p depend on $\mathbf{x}$, t and are assumed to depend on an additional uncertain parameter a, uniformly distributed with μ the mean and σ the standard deviation. In other cases, such as uncertain boundary or initial conditions where the uncertain parameter can naturally follow a normal distribution, the normal distribution is used as discussed in [19]. This parameter a can be an input parameter or the initial or boundary condition. The external force $\mathbf{f}$ is stationary and depends only on $\mathbf{x}$ and a. In PCM the uncertain variables can be decomposed on a basis of orthogonal polynomials, the so-called PCE [18,35,36]. The variable $Y(\mathbf{x},t;a)$ can then be expressed by its PCE

$$Y(\mathbf{x},t;a) = \sum_{i=0}^{n} Y_i(\mathbf{x},t)\psi_i(a). \quad (2)$$

The unknowns, Y_i, are deterministic coefficients representing the random mode i of the physical variable Y, and ψ_i are the orthogonal polynomials of degree i. In the present work, only first-order sensitivity is considered, i.e., $n = 1$. Orthogonality means that

$$\langle \psi_i, \psi_j \rangle = \langle \psi_i, \psi_i \rangle \delta_{ij}, \quad (3)$$

where $\langle \cdot, \cdot \rangle$ denotes the inner product

$$\langle \psi_i, \psi_j \rangle = \langle \psi_i \psi_j \rangle \equiv \int w(a)\psi_i(a)\psi_j(a)da, \quad (4)$$

w is the weighting function and δ_{ij} is the Kronecker delta. If $\langle \psi_i, \psi_i \rangle = 1$, the polynomials are called orthonormal. The optimal polynomials $\psi_0(a)$ and $\psi_1(a)$ for the random variable a are given in this section. For this purpose the weighting function $w(a)$ is considered to be the Probability Density Function (PDF) of the distribution of a. In Section 4 the product of three orthogonal polynomials is used and it is defined as follows

$$\langle \psi_i \psi_j \psi_k \rangle \equiv \int w(a)\psi_i(a)\psi_j(a)\psi_k(a)da.$$

The viscosity ν is spatially and temporally constant, it depends only on a. In what follows ν is uniformly distributed. The choice of the uniform distribution is due to the fact that ν is small and positive thus it cannot follow distributions over negative or large intervals. In terms of mean μ and variance σ^2, the probability density function of the continuous uniform distribution is

$$w(a) = \begin{cases} \dfrac{1}{2\sqrt{3}\sigma} & if \quad a \in [-\sqrt{3}\sigma + \mu, \sqrt{3}\sigma + \mu], \\ 0 & \text{otherwise}, \end{cases}$$

with $-\sqrt{3}\sigma + \mu$ and $\sqrt{3}\sigma + \mu$ positive. To find the first-order sensitivity of the Navier–Stokes equations, Eq. (1), firstly, the polynomials $\psi_0(a)$ and $\psi_1(a)$ are calculated. Let $\psi_0(a) = \alpha$ and $\psi_1(a) = \beta a + \gamma$ be two orthonormal polynomials with α, β, and $\gamma \in \mathbb{R}$. Using the inner product Eq. (4) yields

$$\langle \psi_0, \psi_0 \rangle = \int_{\mathbb{R}} \psi_0(a)\psi_0(a)w(a)da = 1 \Longrightarrow \int_{-\sqrt{3}\sigma+\mu}^{\sqrt{3}\sigma+\mu} \alpha^2 \frac{1}{2\sigma\sqrt{3}} da = 1,$$
$$\Longrightarrow \alpha = 1.$$

Therefore $\psi_0(a) = 1$. Then to compute ψ_1, the inner product of ψ_0 and ψ_1 is calculated as follows

$$\langle \psi_0, \psi_1 \rangle = \int_{\mathbb{R}} \psi_0(a)\psi_1(a)w(a)da = 0 \Longrightarrow \int_{-\sqrt{3}\sigma+\mu}^{\sqrt{3}\sigma+\mu} (\beta a + \gamma) da = 0,$$
$$\Longrightarrow \gamma = -\beta\mu,$$

thus $\psi_1(a) = \beta(a - \mu)$. It remains to find the value of β, thus $\langle \psi_1, \psi_1 \rangle$ is computed

$$\langle \psi_1, \psi_1 \rangle = \int_{\mathbb{R}} \psi_1(a)\psi_1(a)w(a)da = 1, \Longrightarrow \frac{1}{2\sigma\sqrt{3}} \int_{-\sqrt{3}\sigma+\mu}^{\sqrt{3}\sigma+\mu} \beta^2(a-\mu)^2 da = 1.$$
$$\Longrightarrow \beta = \frac{1}{\sigma}.$$

Therefore $\psi_1(a) = \frac{a-\mu}{\sigma}$. Secondly, the variables, i.e., the velocity $\mathbf{u}$, the pressure p, the external force $\mathbf{f}$ and the viscosity ν are expressed by their PCE. Thirdly, these quantities are all inserted in Eq. (1). Then each equation of this system is multiplied by ψ_i (for $i = 0$ and $i = 1$), and to obtain the sensitivity equations the inner product is used.

3.2. Multivariate PCM

The PCM can be extended to multivariate independent random variables, where the orthogonal multivariate polynomials are the product of the constructed univariate orthogonal polynomials. The same orthogonalization approach for univariate polynomials is used to construct directly a multidimensional orthogonal polynomial basis $\{\phi_i(\mathbf{a})\}$, for multivariate random input variables. Let $\mathbf{a} = (a_0, \dots, a_{d-1}) \in \mathbb{R}^d$ a vector of independent random variables, with joint PDF $\boldsymbol{w}(\mathbf{a})$. The parameter $\mathbf{a}$ contains the uncertainties in the model's initial or boundary conditions and the input parameters. Let $Y(\mathbf{x}, t; \mathbf{a})$ be an uncertain variable that depends on space $\mathbf{x}$, time t and an uncertain vector $\mathbf{a}$. In multivariate PCM, the uncertain variables can be decomposed on the basis of complete multivariate orthogonal polynomials, the so-called multivariate PCE [32,37]. The variable $Y(\mathbf{x}, t; \mathbf{a})$ can then be expressed by its multivariate PCE

$$Y(\mathbf{x}, t; \mathbf{a}) = \sum_{i=0}^{d} Y_i(\mathbf{x}, t)\phi_i(\mathbf{a}). \tag{5}$$

The unknowns, Y_i, are deterministic coefficients and represent the random mode i of the physical variable component Y, and ϕ_i are the multivariate orthogonal polynomials of degree at most i. The polynomials ϕ_0 and ϕ_1 are defined in $\mathbb{R}^d$ and take value in $\mathbb{R}$. Due to the independence of the elements $a_0, \dots, a_{d-1}$, the multivariate polynomials ϕ_0 and ϕ_1 can be constructed using the univariate polynomial basis as follows

$$\phi_0(\mathbf{a}) = \prod_{i=0}^{d-1} \psi_0(a_i) = 1,$$
$$\phi_1(\mathbf{a}) = \psi_1(a_0) \prod_{i}^{d-1} \psi_0(a_i) = \psi_1(a_0),$$
$$\vdots$$
$$\phi_d(\mathbf{a}) = \psi_1(a_{d-1}) \prod_{i=0}^{d-2} \psi_0(a_i) = \psi_1(a_{d-1}),$$

with $\psi_j(a_i)$ denotes the univariate orthogonal polynomials. The index j is the polynomial degree of $\psi_j(a_i)$. The type of the univariate polynomial $\psi_j(a_i)$ depends on the input variable a_i distribution. For instance, the Legendre, Hermite, or Laguerre polynomial function is selected as the orthogonal polynomial function if the input variable follows uniform, normal, or gamma distribution, respectively. In this work, only the multivariate polynomials of degree at most 1 are computed, see [38] for the computation of multivariate polynomials of higher degree. The Galerkin projection is used to compute the polynomial chaos expansion coefficients a_i and Y_i (as in Section 3.1). Due to the independence of the uncertain parameters $a_0, \dots, a_{d-1}$, d systems are obtained.

In Section 6 the lid-driven cavity numerical test is treated with both univariate and multivariate uncertain parameters.

3.3. Uncertainty quantification

The PCE provides an easy way to compute the mean and the standard deviation of the uncertain variable Y using the expansion coefficients. The mean and the standard deviation of the uncertain variable Y are written as follows

$$\mu_Y^a(\mathbf{x}, t) = E\left(Y(\mathbf{x}, t)\right) = E\left(Y_0(\mathbf{x}, t) + \frac{a-\mu}{\sigma} Y_1(\mathbf{x}, t)\right) = Y_0(\mathbf{x}, t), \text{ and} \tag{6}$$

$$\sigma_Y^a(\mathbf{x}, t) = E\Big(\big(Y(\mathbf{x}, t) - Y_0(\mathbf{x}, t)\big)^2\Big)$$
$$= E\Big(\big(\sum_{i=0}^{n} Y_i(\mathbf{x}, t)\psi_i(a) - Y_0(\mathbf{x}, t)\big)^2\Big) = \sum_{i=1}^{n} Y_i^2(\mathbf{x}, t). \tag{7}$$

4. Sensitivity of the Navier–Stokes equations

In this section, the PCM is applied to the Navier–Stokes equations, Eq. (1). For the clarity of further mathematical manipulations, we expand the equations under the following form

$$\begin{cases} u_t - \nu(u_{xx} + u_{yy}) + uu_x + vu_y + p_x = f^x & \Omega, t > 0, \quad (8a) \\ v_t - \nu(v_{xx} + v_{yy}) + uv_x + vv_y + p_y = f^y & \Omega, t > 0, \quad (8b) \\ u_x + v_y = 0 & \Omega, t > 0, \quad (8c) \\ u(\mathbf{x}, 0) = 0 & \Omega, t = 0, \quad (8d) \\ v(\mathbf{x}, 0) = 0 & \Omega, t = 0, \quad (8e) \\ u(\mathbf{x}, t) = g^x(\mathbf{x}, t) & \Gamma, t > 0. \quad (8f) \\ v(\mathbf{x}, t) = g^y(\mathbf{x}, t) & \Gamma, t > 0. \quad (8g) \end{cases}$$

The subscripts x and y refer to spatial derivatives, specifically first partial derivatives, with xx and yy denoting second partial derivatives with respect to space, while the subscript t signifies temporal derivatives.

The PCE of the two scalar components of the velocity, and the external force are respectively written as follows

$$u(\mathbf{x},t;a)=\sum_{i=0}^{1}u_i(\mathbf{x},t)\psi_i(a),\quad v(\mathbf{x},t;a)=\sum_{i=0}^{1}v_i(\mathbf{x},t)\psi_i(a)$$
$$f^x(\mathbf{x};a)=\sum_{i=0}^{1}f_i^x(\mathbf{x})\psi_i(a),\quad f^y(\mathbf{x};a)=\sum_{i=0}^{1}f_i^y(\mathbf{x})\psi_i(a)$$

and the PCE of the pressure and the viscosity are presented respectively as follows

$$p(\mathbf{x},t;a)=\sum_{i=0}^{1}p_i(\mathbf{x},t)\psi_i(a),\quad \nu(a)=\sum_{i=0}^{1}\nu_i\psi_i(a).$$

The PCE of the boundary condition is written as follows

$$\mathbf{g}^x(\mathbf{x},t;a)=\sum_{i=0}^{1}\mathbf{g}_i^x(\mathbf{x},t)\psi_i(a),\quad \mathbf{g}^y(\mathbf{x};a)=\sum_{i=0}^{1}\mathbf{g}_i^y(\mathbf{x})\psi_i(a).$$

We replace in Eqs. (8a)–(8g), the two scalar components of the velocity and the external force, the pressure, and the viscosity by their PCE. A spectral stochastic projection is performed by multiplying Eqs. (8a)–(8g) with ψ_k for $k=\{0,1\}$ and integrating with regard to the PDF $w(a)$. The equations deduced from Eqs. (8a)–(8g) are

$$\begin{cases}
(u_k)_t-\sum_{i=0}^{1}\sum_{j=0}^{1}\nu_i[(u_j)_{xx}+(u_j)_{yy}]\langle\psi_i\psi_j\psi_k\rangle & \\
+\sum_{i=0}^{1}\sum_{j=0}^{1}[u_i(u_j)_x+v_i(u_j)_y]\langle\psi_i\psi_j\psi_k\rangle+(p_k)_x=f_k^x & \Omega,\ t>0, \quad (9a)\\
(v_k)_t-\sum_{i=0}^{1}\sum_{j=0}^{1}\nu_i[(v_j)_{xx}+(v_j)_{yy}]\langle\psi_i\psi_j\psi_k\rangle & \\
+\sum_{i=0}^{1}\sum_{j=0}^{1}[u_i(v_j)_x+v_i(v_j)_y]\langle\psi_i\psi_j\psi_k\rangle+(p_k)_y=f_k^y & \Omega,\ t>0, \quad (9b)\\
(u_k)_x+(v_k)_y=0 & \Omega,\ t>0, \quad (9c)\\
u_k(\mathbf{x},0)=0 & \Omega,\ t=0, \quad (9d)\\
v_k(\mathbf{x},0)=0 & \Omega,\ t=0, \quad (9e)\\
u_k(\mathbf{x},t)=g_k^x(\mathbf{x},t) & \Gamma,\ t>0. \quad (9f)\\
v_k(\mathbf{x},t)=g_k^y(\mathbf{x},t) & \Gamma,\ t>0. \quad (9g)
\end{cases}$$

Let $\mathbf{u}^s=(u_0,u_1)^t$, $\mathbf{v}^s=(v_0,v_1)^t$, $\mathbf{p}^s=(p_0,p_1)^t$, $(\mathbf{f}^s)^x=(f_0^x,f_1^x)$, $(\mathbf{f}^s)^y=(f_0^y,f_1^y)$, $\boldsymbol{\nu}^s=(\nu_0,\nu_1)^t$, and $(\mathbf{g}^s)^x=(g_0^x,g_1^x)$, $(\mathbf{g}^s)^y=(g_0^y,g_1^y)$ denote the vectors of PC coefficients of u, v, p, f^x, f^y, ν, g^x, and g^y respectively. To write the Eqs. (9a)–(9g) in a more compact way, we define the matrix $A(\mathbf{b})$ with $\mathbf{b}=(b^0,b^1)\in\mathbb{R}^2$, as follows

$$[A(\mathbf{b})]_{kj}=\sum_{i=0}^{1}b_i\langle\psi_i\psi_j\psi_k\rangle,\quad j,k\in\{0,1\}.$$

By the definition of $A(\cdot)$, for any vector $\boldsymbol{b}$, $\boldsymbol{c}\in\mathbb{R}^2$, it yields that

$$[A(\boldsymbol{b})\boldsymbol{c}]_k=\sum_{i=0}^{1}\sum_{j=0}^{1}\langle\psi_i\psi_j\psi_k\rangle b_ic_j=\sum_{i=0}^{1}\sum_{j=0}^{1}\langle\psi_i\psi_j\psi_k\rangle b_jc_i=[A(\boldsymbol{c})\boldsymbol{b}]_k.$$

Thus, one has

$$A(\boldsymbol{b})\boldsymbol{c}=A(\boldsymbol{c})\boldsymbol{b}. \quad (10)$$

By replacing these vectors and matrices in Eqs. (9a)–(9g), it yields

$$\begin{cases}
\mathbf{u}_t^s-A(\boldsymbol{\nu}^s)[\mathbf{u}_{xx}^s+\mathbf{u}_{yy}^s]+A(\mathbf{u}^s)\mathbf{u}_x^s+A(\mathbf{v}^s)\mathbf{u}_y^s+\mathbf{p}_x^s=(\mathbf{f}^s)^x & \Omega,\ t>0, \quad (11a)\\
\mathbf{v}_t^s-A(\boldsymbol{\nu}^s)[\mathbf{v}_{xx}^s+\mathbf{v}_{yy}^s]+A(\mathbf{u}^s)\mathbf{v}_x^s+A(\mathbf{v}^s)\mathbf{v}_y^s+\mathbf{p}_y^s=(\mathbf{f}^s)^y & \Omega,\ t>0, \quad (11b)\\
\mathbf{u}_x^s+\mathbf{v}_y^s=\mathbf{0} & \Omega,\ t>0, \quad (11c)\\
\mathbf{u}^s(\mathbf{x},0)=\mathbf{0} & \Omega,\ t=0, \quad (11d)\\
\mathbf{v}^s(\mathbf{x},0)=\mathbf{0} & \Omega,\ t=0, \quad (11e)\\
\mathbf{u}^s(\mathbf{x},t)=(\mathbf{g}^s)^x & \Gamma,\ t>0. \quad (11f)\\
\mathbf{v}^s(\mathbf{x},t)=(\mathbf{g}^s)^y & \Gamma,\ t>0. \quad (11g)
\end{cases}$$

Proposition 1. *If $\nu(a)w(a)>0$, then the matrix $A(\boldsymbol{\nu}^s)$ is definite positive [39,40].*

Proof. Let $\mathbf{b}=(b_0,b_1)^t\in\mathbb{R}^2$ an arbitrary real vector and $b(a)=\sum_{j=0}^{1}b_j\psi_j(a)$. Then

$$\begin{aligned}\mathbf{b}^tA(\boldsymbol{\nu}^s)\mathbf{b}&=\sum_{i=0}^{1}\sum_{j=0}^{1}\sum_{k=0}^{1}b_j\left(\int_{\mathbb{R}}\nu_i\psi_i(a)\psi_j(a)\psi_k(a)w(a)\,da\right)b_k\\&=\int_{\mathbb{R}}\nu(a)(b_0+b_1)^2w(a)\,da. \quad (12)\end{aligned}$$

Since $\nu(a)w(a)\geq 0$, one has

$$\mathbf{b}^tA(\boldsymbol{\nu}^s)\mathbf{b}=\int_{\mathbb{R}}\nu(a)(b_0+b_1)^2w(a)\,da>0,$$

thus the matrix $A(\boldsymbol{\nu}^s)$ is definite positive for all $\mathbf{b}\in\mathbb{R}^2$. □

A stability estimate is presented in what follows. To simplify the proof, homogeneous Dirichlet boundary conditions, i.e., $\mathbf{g}(\mathbf{x},t)=0$ in Eq. (1), will be assumed.

Proposition 2. *If $A(\boldsymbol{\nu}^s)$ is definite positive and $\mathbf{f}=(f^x,f^y)$ stationary, then*

$$\begin{aligned}&\|\mathbf{u}^s\|^2+\|\mathbf{v}^s\|^2+2\int_0^t\Big(\|\mathbf{u}_x^s(r)\|^2_{A(\boldsymbol{\nu}^s)}+\|\mathbf{u}_y^s(r)\|^2_{A(\boldsymbol{\nu}^s)}+\|\mathbf{v}_x^s(r)\|^2_{A(\boldsymbol{\nu}^s)}\\&+\|\mathbf{v}_y^s(r)\|^2_{A(\boldsymbol{\nu}^s)}+\|\mathbf{u}_x^s(r)\|^2_{A(\boldsymbol{\nu}^s)}\Big)\,dr\\&\leq(e^{-t}-1)(\|(\mathbf{f}^s)^x\|^2+\|(\mathbf{f}^s)^y\|^2). \quad (13)\end{aligned}$$

with $\|\cdot\|$ the L^2- norm in space and $\|\cdot\|_{A(\boldsymbol{\nu}^s)}$ the norm induced by the matrix $A(\boldsymbol{\nu}^s)$.

In what follows the norm induced by the matrix $A(\boldsymbol{\nu}^s)$ is defined as follows

Let $\mathbf{u}\in\mathbb{R}^2$, $\|\mathbf{u}\|_{A(\boldsymbol{\nu}^s)}=\int_\Omega\mathbf{u}^t[A(\boldsymbol{\nu}^s)\mathbf{u}]\,d\mathbf{x}$.

Proof. The stability estimate Eq. (13) is obtained by multiplying Eq. (11a) by $(\mathbf{u}^s)^t$ and Eq. (11b) by $(\mathbf{v}^s)^t$. Then the sum of the two equations is integrated over the spatial space and multiplied by 2. The resulting expression can be written as follows

$$\begin{aligned}&\frac{d}{dt}(\|\mathbf{u}^s\|^2+\|\mathbf{v}^s\|^2)+2\int_\Omega(\mathbf{u}^s)^tA(\mathbf{u}^s)\mathbf{u}_x^s+(\mathbf{v}^s)^tA(\mathbf{u}^s)\mathbf{v}_x^s\\&+(\mathbf{u}^s)^tA(\mathbf{v}^s)\mathbf{u}_y^s+(\mathbf{v}^s)^tA(\mathbf{v}^s)\mathbf{v}_y^s\,d\mathbf{x}\\&+2\int_\Omega(\mathbf{u}^s)^t\cdot\mathbf{p}_x^s+(\mathbf{v}^s)^t\cdot\mathbf{p}_y^s\,d\mathbf{x}\\&-2\int_\Omega(\mathbf{u}^s)^t[A(\boldsymbol{\nu}^s)\mathbf{u}_{xx}^s]+(\mathbf{u}^s)^t[A(\boldsymbol{\nu}^s)\mathbf{u}_{yy}^s]\\&+(\mathbf{v}^s)^t[A(\boldsymbol{\nu}^s)\mathbf{v}_{xx}^s]+(\mathbf{v}^s)^t[A(\boldsymbol{\nu}^s)\mathbf{v}_{yy}^s]\,d\mathbf{x}\\&=2\int_\Omega(\mathbf{u}^s)^t(\mathbf{f}^s)^x\,d\mathbf{x}+2\int_\Omega(\mathbf{v}^s)^t(\mathbf{f}^s)^y\,d\mathbf{x}. \quad (14)\end{aligned}$$

For clarity, we treat the terms group wise below. First the **advective term** is treated. Knowing that for all $\boldsymbol{b}=(b_0,b_1)\in\mathbb{R}^2$, $A(\boldsymbol{b})$ is symmetric and according to Eq. (10) one has

$$2A(\mathbf{u}^s)\mathbf{u}_x^s=A(\mathbf{u}^s)\mathbf{u}_x^s+A(\mathbf{u}_x^s)\mathbf{u}^s=[A(\mathbf{u}^s)\mathbf{u}^s]_x. \quad (15)$$

By substituting Eq. (15) in the **advective term**, it becomes

$$2\int_\Omega (\mathbf{u}^s)^t A(\mathbf{u}^s)\mathbf{u}^s_x + (\mathbf{v}^s)^t A(\mathbf{u}^s)\mathbf{v}^s_x + (\mathbf{u}^s)^t A(\mathbf{v}^s)\mathbf{u}^s_y + (\mathbf{v}^s)^t A(\mathbf{v}^s)\mathbf{v}^s_y \, d\mathbf{x}$$
$$= \int_\Omega (\mathbf{u}^s)^t [A(\mathbf{u}^s)\mathbf{u}^s]_x + 2(\mathbf{v}^s)^t A(\mathbf{u}^s)\mathbf{v}^s_x + 2(\mathbf{u}^s)^t A(\mathbf{v}^s)\mathbf{u}^s_y + (\mathbf{v}^s)^t [A(\mathbf{v}^s)\mathbf{v}^s]_y \, d\mathbf{x} \tag{16}$$

According to the Eq. (10), Eq. (16) yields

$$2\int_\Omega (\mathbf{u}^s)^t A(\mathbf{u}^s)\mathbf{u}^s_x + (\mathbf{v}^s)^t A(\mathbf{u}^s)\mathbf{v}^s_x + (\mathbf{u}^s)^t A(\mathbf{v}^s)\mathbf{u}^s_y + (\mathbf{v}^s)^t A(\mathbf{v}^s)\mathbf{v}^s_y \, d\mathbf{x}$$
$$= \int_\Omega (\mathbf{u}^s)^t [A(\mathbf{u}^s)\mathbf{u}^s]_x + 2(\mathbf{v}^s)^t A(\mathbf{v}^s_x)\mathbf{u}^s + 2(\mathbf{u}^s)^t A(\mathbf{u}^s_y)\mathbf{v}^s + (\mathbf{v}^s)^t [A(\mathbf{v}^s)\mathbf{v}^s]_y \, d\mathbf{x}. \tag{17}$$

Knowing that the matrix A is symmetric, Eq. (17) rewrites

$$2\int_\Omega (\mathbf{u}^s)^t A(\mathbf{u}^s)\mathbf{u}^s_x + (\mathbf{v}^s)^t A(\mathbf{u}^s)\mathbf{v}^s_x + (\mathbf{u}^s)^t A(\mathbf{v}^s)\mathbf{u}^s_y + (\mathbf{v}^s)^t A(\mathbf{v}^s)\mathbf{v}^s_y \, d\mathbf{x}$$
$$= \int_\Omega (\mathbf{u}^s)^t [A(\mathbf{u}^s)\mathbf{u}^s]_x + 2(\mathbf{u}^s)^t A(\mathbf{v}^s_x)\mathbf{v}^s + 2(\mathbf{v}^s)^t A(\mathbf{u}^s_y)\mathbf{u}^s + (\mathbf{v}^s)^t [A(\mathbf{v}^s)\mathbf{v}^s]_y \, d\mathbf{x}. \tag{18}$$

According to the Eq. (15), Eq. (18) simplifies to

$$2\int_\Omega (\mathbf{u}^s)^t A(\mathbf{u}^s)\mathbf{u}^s_x + (\mathbf{v}^s)^t A(\mathbf{u}^s)\mathbf{v}^s_x + (\mathbf{u}^s)^t A(\mathbf{v}^s)\mathbf{u}^s_y + (\mathbf{v}^s)^t A(\mathbf{v}^s)\mathbf{v}^s_y \, d\mathbf{x}$$
$$= \int_\Omega (\mathbf{u}^s)^t [A(\mathbf{u}^s)\mathbf{u}^s + A(\mathbf{v}^s)\mathbf{v}^s]_x + (\mathbf{v}^s)^t [A(\mathbf{u}^s)\mathbf{u}^s + A(\mathbf{v}^s)\mathbf{v}^s]_y \, d\mathbf{x}. \tag{19}$$

Let $\boldsymbol{n} = (n_1, n_2)$ be the normal vector. By integrating by part Eq. (19), one has

$$2\int_\Omega (\mathbf{u}^s)^t [A(\mathbf{u}^s)\mathbf{u}^s_x + (\mathbf{v}^s)^t A(\mathbf{u}^s)\mathbf{v}^s_x] + (\mathbf{u}^s)^t [A(\mathbf{v}^s)\mathbf{u}^s_y + (\mathbf{v}^s)^t A(\mathbf{v}^s)\mathbf{v}^s_y] \, d\mathbf{x}$$
$$= -\int_\Omega (\mathbf{u}^s_x + \mathbf{v}^s_y)^t [A(\mathbf{u}^s)\mathbf{u}^s + A(\mathbf{v}^s)\mathbf{v}^s] \, d\mathbf{x} + \int_\Gamma (\mathbf{u}^s n_1 + \mathbf{v}^s n_2)^t [A(\mathbf{u}^s)\mathbf{u}^s + A(\mathbf{v}^s)\mathbf{v}^s] \, dS. \tag{20}$$

According to the Eq. (11c) and to the homogeneous Dirichlet boundary condition, Eq. (20) becomes

$$2\int_\Omega (\mathbf{u}^s)^t [A(\mathbf{u}^s)\mathbf{u}^s_x + (\mathbf{v}^s)^t A(\mathbf{u}^s)\mathbf{v}^s_x] + (\mathbf{u}^s)^t [A(\mathbf{v}^s)\mathbf{u}^s_y + (\mathbf{v}^s)^t A(\mathbf{v}^s)\mathbf{v}^s_y] \, d\mathbf{x} = 0. \tag{21}$$

By integrating by part the **pressure term** and according to the Eq. (11c) and to the homogeneous Dirichlet boundary condition, it gives

$$2\int_\Omega (\mathbf{u}^s)^t \cdot \mathbf{p}^s_x + (\mathbf{v}^s)^t \cdot \mathbf{p}^s_y \, d\mathbf{x} = -2\int_\Omega (\mathbf{u}^s_x + \mathbf{v}^s_y)^t \mathbf{p}^s \, d\mathbf{x} + 2\int_\Gamma (\mathbf{u}^s n_1 + \mathbf{v}^s n_2)^t \mathbf{p}^s \, dS = 0. \tag{22}$$

The **diffusive term** is treated using an integration by part as follows

$$-2\int_\Omega (\mathbf{u}^s)^t [A(\nu^s)\mathbf{u}^s_{xx}] + (\mathbf{u}^s)^t [A(\nu^s)\mathbf{u}^s_{yy}]$$
$$+ (\mathbf{v}^s)^t [A(\nu^s)\mathbf{v}^s_{xx}] + (\mathbf{v}^s)^t [A(\nu^s)\mathbf{v}^s_{yy}] \, d\mathbf{x}$$
$$= 2\int_\Omega (\mathbf{u}^s_x)^t [A(\nu^s)\mathbf{u}^s_x] + (\mathbf{u}^s_y)^t [A(\nu^s)\mathbf{u}^s_y]$$
$$+ (\mathbf{v}^s_x)^t [A(\nu^s)\mathbf{v}^s_x] + (\mathbf{v}^s_y)^t [A(\nu^s)\mathbf{v}^s_y] \, d\mathbf{x}$$
$$- 2\int_\Gamma n_1 (\mathbf{u}^s)^t [A(\nu^s)\mathbf{u}^s_x] + n_2 (\mathbf{u}^s)^t [A(\nu^s)\mathbf{u}^s_y]$$
$$+ n_1 (\mathbf{v}^s)^t [A(\nu^s)\mathbf{v}^s_x] + n_2 (\mathbf{v}^s_x)^t [A(\nu^s)\mathbf{v}^s_y] \, dS. \tag{23}$$

According to the boundary conditions Eqs. (11f)–(11g), Eq. (23) becomes

$$-2\int_\Omega (\mathbf{u}^s)^t [A(\nu^s)\mathbf{u}^s_{xx}] + (\mathbf{u}^s)^t [A(\nu^s)\mathbf{u}^s_{yy}] + (\mathbf{v}^s)^t [A(\nu^s)\mathbf{v}^s_{xx}] + (\mathbf{v}^s)^t [A(\nu^s)\mathbf{v}^s_{yy}] \, d\mathbf{x}$$
$$= 2(\|\mathbf{u}^s_x\|^2_{A(\nu^s)} + \|\mathbf{u}^s_y\|^2_{A(\nu^s)} + \|\mathbf{v}^s_x\|^2_{A(\nu^s)} + \|\mathbf{v}^s_y\|^2_{A(\nu^s)} + \|\mathbf{u}^s_x\|^2_{A(\nu^s)}). \tag{24}$$

By applying the Cauchy–Schwarz and Young inequalities to the **right-hand side** of Eq. (14), one has

$$2\int_\Omega (\mathbf{u}^s)^t (\mathbf{f}^s)^x \, d\mathbf{x} + 2\int_\Omega (\mathbf{v}^s)^t (\mathbf{f}^s)^y \, d\mathbf{x} \le 2(\|\mathbf{u}^s\| \|(\mathbf{f}^s)^x\| + \|\mathbf{v}^s\| \|(\mathbf{f}^s)^y\|)$$
$$\le \|\mathbf{u}^s\|^2 + \|(\mathbf{f}^s)^x\|^2 + \|\mathbf{v}^s\|^2 + \|(\mathbf{f}^s)^y\|^2. \tag{25}$$

By replacing all these inequalities Eq. (20), Eq. (22), Eq. (24), and Eq. (25) in Eq. (14), it gives

$$\frac{d}{dt}(\|\mathbf{u}^s\|^2 + \|\mathbf{v}^s\|^2) + 2(\|\mathbf{u}^s_x\|^2_{A(\nu^s)} + \|\mathbf{u}^s_y\|^2_{A(\nu^s)} + \|\mathbf{v}^s_x\|^2_{A(\nu^s)} + \|\mathbf{v}^s_y\|^2_{A(\nu^s)})$$
$$\le \|\mathbf{u}^s\|^2 + \|(\mathbf{f}^s)^x\|^2 + \|\mathbf{v}^s\|^2 + \|(\mathbf{f}^s)^y\|^2. \tag{26}$$

By integrating Eq. (26) in time, one has

$$\|\mathbf{u}^s\|^2 + \|\mathbf{v}^s\|^2 + 2\int_0^t \left(\|\mathbf{u}^s_x(r)\|^2_{A(\nu^s)} + \|\mathbf{u}^s_y(r)\|^2_{A(\nu^s)} + \|\mathbf{v}^s_x(r)\|^2_{A(\nu^s)} + \|\mathbf{v}^s_y(r)\|^2_{A(\nu^s)}\right) dr$$
$$\le \int_0^t \|\mathbf{u}^s(r)\|^2 + \|\mathbf{v}^s(r)\|^2 \, dr + t\left(\|(\mathbf{f}^s)^x\|^2 + \|(\mathbf{f}^s)^y\|^2\right). \tag{27}$$

By setting $z(t) = \int_0^t \|\mathbf{u}^s(r)\|^2 + \|\mathbf{v}^s(r)\|^2 \, dr$ and replacing it in Eq. (27) and knowing that $2\int_0^t \left(\|\mathbf{u}^s_x(r)\|^2_{A(\nu^s)} + \|\mathbf{u}^s_y(r)\|^2_{A(\nu^s)} + \|\mathbf{v}^s_x(r)\|^2_{A(\nu^s)} + \|\mathbf{v}^s_y(r)\|^2_{A(\nu^s)}\right) dr$ is positive, one has

$$z'(t) \le z(t) + t(\|(\mathbf{f}^s)^x\|^2 + \|(\mathbf{f}^s)^y\|^2). \tag{28}$$

By multiplying Eq. (28) by e^{-t}, it gives

$$(e^{-t} z(t))' \le e^{-t} t(\|(\mathbf{f}^s)^x\|^2 + \|(\mathbf{f}^s)^y\|^2). \tag{29}$$

Integrating in time Eq. (29) and multiplying it by e^t, one has

$$z(t) \le (e^t - 1 - t)(\|(\mathbf{f}^s)^x\|^2 + \|(\mathbf{f}^s)^y\|^2). \tag{30}$$

Finally, $z(t)$ is replaced in Eq. (27), the following inequality holds

$$\|\mathbf{u}^s\|^2 + \|\mathbf{v}^s\|^2 + 2\int_0^t (\|\mathbf{u}^s_x(r)\|^2_{A(\nu^s)} + \|\mathbf{u}^s_y(r)\|^2_{A(\nu^s)}$$
$$+ \|\mathbf{v}^s_x(r)\|^2_{A(\nu^s)} + \|\mathbf{v}^s_y(r)\|^2_{A(\nu^s)}) \, dr$$
$$\le (e^t - 1)(\|(\mathbf{f}^s)^x\|^2 + \|(\mathbf{f}^s)^y\|^2). \quad \square \tag{31}$$

The interested reader can refer to [41] for an adaptation to mixed non-homogeneous boundary conditions.

5. Decoupling and numerical computation of the sensitivity equations

In this section, we want to find a way to solve the stochastic Navier–Stokes equations. For this purpose, the Navier–Stokes equations Eq. (1) are considered. Then, the first-order intrusive PCM is applied to these equations. First, the method is applied for $i = 0$, and the following equations are obtained

$$\begin{cases} \partial_t \mathbf{u}_0(\mathbf{x},t) - \nu_0 \Delta \mathbf{u}_0(\mathbf{x},t) - \nu_1 \Delta \mathbf{u}_1(\mathbf{x},t) + (\mathbf{u}_0(\mathbf{x},t)\cdot\nabla)\mathbf{u}_0(\mathbf{x},t) & \\ \quad + (\mathbf{u}_1(\mathbf{x},t)\cdot\nabla)\mathbf{u}_1(\mathbf{x},t) + \nabla p_0(\mathbf{x},t) = \mathbf{f}_0(\mathbf{x}) & \Omega, t>0, \\ \nabla\cdot\mathbf{u}_0(\mathbf{x},t) = \mathbf{0} & \Omega, t>0, \\ \mathbf{u}_0(\mathbf{x},0) = \mathbf{0} & \Omega, t=0, \\ \mathbf{u}_0(\mathbf{x},t) = \mathbf{g}_0(\mathbf{x},t) & \Gamma, t>0. \end{cases} \tag{32}$$

These equations are equivalent to Eqs. (9a)–(9g) for $i = 0$. Second, the Navier–Stokes Eq. (1) are multiplied by ψ_1 and the inner product is applied. Then, the obtained equations are grouped in the following system

$$\begin{cases} \partial_t \mathbf{u}_1(\mathbf{x},t) - \nu_0 \Delta \mathbf{u}_1(\mathbf{x},t) - \nu_1 \Delta \mathbf{u}_0(\mathbf{x},t) + (\mathbf{u}_0(\mathbf{x},t)\cdot\nabla)\mathbf{u}_1(\mathbf{x},t) & \\ \quad + (\mathbf{u}_1(\mathbf{x},t)\cdot\nabla)\mathbf{u}_0(\mathbf{x},t) + \nabla p_1(\mathbf{x},t) = \mathbf{f}_1(\mathbf{x}) & \Omega, t>0, \\ \nabla\cdot\mathbf{u}_1(\mathbf{x},t) = \mathbf{0} & \Omega, t>0, \\ \mathbf{u}_1(\mathbf{x},0) = \mathbf{0} & \Omega, t=0, \\ \mathbf{u}_1(\mathbf{x},t) = \mathbf{g}_1(\mathbf{x},t) & \Gamma, t>0. \end{cases} \tag{33}$$

$$
\begin{cases}
\partial_t \tilde{\mathbf{u}}_1(\mathbf{x},t) - \tilde{\nu}_0 \Delta \tilde{\mathbf{u}}_1(\mathbf{x},t) - \tilde{\nu}_1 \Delta \tilde{\mathbf{u}}_0(\mathbf{x},t) - 2\sigma \tilde{\nu}_1 \Delta \tilde{\mathbf{u}}_1(\mathbf{x},t) + (\tilde{\mathbf{u}}_0(\mathbf{x},t)\cdot\nabla)\tilde{\mathbf{u}}_1(\mathbf{x},t) & \\
\quad + (\tilde{\mathbf{u}}_1(\mathbf{x},t)\cdot\nabla)\tilde{\mathbf{u}}_0(\mathbf{x},t) + 2\sigma(\tilde{\mathbf{u}}_1(\mathbf{x},t)\cdot\nabla)\tilde{\mathbf{u}}_1(\mathbf{x},t) + \nabla\tilde{p}_1 = \tilde{\mathbf{f}}_1(\mathbf{x}) & \Omega, t>0,\\
\nabla\cdot\tilde{\mathbf{u}}_1(\mathbf{x},t) = \mathbf{0} & \Omega, t>0,\\
\tilde{\mathbf{u}}_1(\mathbf{x},0) = \mathbf{0} & \Omega, t=0,\\
\tilde{\mathbf{u}}_1(\mathbf{x},t) = \tilde{\mathbf{g}}_1(\mathbf{x},t) & \Gamma,\ t>0.
\end{cases} \tag{35}
$$

Box I.

These equations are equivalent to Eqs. (9a)–(9g) for $i = 1$. One can notice that this intrusive approach results in a coupled system of advection–diffusion equations for the stochastic velocity fields and a decoupled set of stochastic divergence constraints. Therefore, this makes them difficult to solve numerically. Some methods are proposed to simplify the resolution of these two systems, like the Stochastic Projection Method (SPM), in [42,43]. This approach is based on the observation that the velocity divergence constraints are decoupled. It suggests implementing a projection scheme in which the advection and diffusion terms are integrated in a first fractional step, and the divergence constraints are then enforced in a second fractional step.

Since the two systems, Eqs. (32) and (33), are coupled, it is fortunate that they can be decoupled. Decoupling results in two systems, one of which is the Navier–Stokes system, which is advantageous for implementation in pre-existing code. This paper proposes an approach involving decoupling, where two equivalent systems of other partial differential equations (PDEs) are identified. This approach ensures that one of the systems does not depend on the solution of the second system (i.e. the global system is triangular). This is done using the following change of variables

$$\mathbf{u}_1 = \sigma\tilde{\mathbf{u}}_1, \quad p_1 = \sigma\tilde{p}_1, \quad \nu_1 = \sigma\tilde{\nu}_1, \mathbf{f}_1 = \sigma\tilde{\mathbf{f}}_1, \text{ and } \mathbf{g}_1 = \sigma\tilde{\mathbf{g}}_1,$$

then these quantities are inserted in system (33). This new system (33) is subtracted from system (32) and according to the following change of variables

$$\mathbf{u}_0 = \tilde{\mathbf{u}}_0 + \sigma\tilde{\mathbf{u}}_1, \quad p_0 = \tilde{p}_0 + \sigma\tilde{p}_1, \quad \nu_0 = \tilde{\nu}_0 + \sigma\tilde{\nu}_1,$$
$$\mathbf{f}_0 = \tilde{\mathbf{f}}_0 + \sigma\tilde{\mathbf{f}}_1, \text{ and } \mathbf{g}_0 = \tilde{\mathbf{g}}_0 + \sigma\tilde{\mathbf{g}}_1.$$

Finally, two decoupled systems (34) and (35) equivalent to the systems (32) and (33) are obtained

$$
\begin{cases}
\partial_t \tilde{\mathbf{u}}_0(\mathbf{x},t) - \tilde{\nu}_0 \Delta \tilde{\mathbf{u}}_0(\mathbf{x},t) + (\tilde{\mathbf{u}}_0(\mathbf{x},t)\cdot\nabla)\tilde{\mathbf{u}}_0(\mathbf{x},t) + \nabla\tilde{p}_0(\mathbf{x},t) = \tilde{\mathbf{f}}_0(\mathbf{x}) & \Omega, t>0,\\
\nabla\cdot\tilde{\mathbf{u}}_0(\mathbf{x},t) = \mathbf{0} & \Omega, t>0,\\
\tilde{\mathbf{u}}_0(\mathbf{x},0) = \mathbf{0} & \Omega, t=0,\\
\tilde{\mathbf{u}}_0(\mathbf{x},t) = \tilde{\mathbf{g}}_0(\mathbf{x},t) & \Gamma, t>0,
\end{cases} \tag{34}
$$

with $\tilde{\mathbf{u}}_0$, $\tilde{p}_0$ and $\tilde{\mathbf{f}}_0$ the velocity, pressure and external force respectively.

The system (34) corresponds to the Navier–Stokes Eq. (1). The system (35) (see Box I) represents the first-order sensitivity of the Navier–Stokes equations, with $\tilde{\mathbf{u}}_1$, $\tilde{p}_1$, and $\tilde{\mathbf{f}}_1$ the sensitivity of the velocity, pressure, and external force respectively. These equations will also be referred to as sensitivity equations in the following. The system (35) can be solved once system (34) is solved and the value of $\tilde{\mathbf{u}}_0$ is computed. One can note that the mean and standard deviation of an uncertain variable (Section 3.3) are computed based on the state and sensitivity using just two simulations: the first to compute the Navier–Stokes Eqs. (34) and the second to compute the first-order sensitivity of the Navier–Stokes Eqs. (35).

6. Numerical results

This section presents a numerical test, the lid-driven cavity, already performed in [35,44], see [19] for other numerical results treated using the IPCM. The sensitivity of the Navier–Stokes equations of the corresponding test, the average and the standard deviation of the uncertain variables are computed according to the PCM, and compared to the one obtained in [44] and the ones obtained using the Taylor expansion [41,45]. The mean and the standard deviation are computed using Eqs. (6)– (7) and the change of variable presented in Section 5.

Let $\Omega = [0,1]\times[0,1]$ be a $2d$ square cavity of which the upper wall is moving with a velocity $\mathbf{u} = (1,0)$. The flow is laminar with $Re = 100$. In what follows, scenarios are presented: one with uncertain viscosity and boundary conditions and the third one with both uncertain viscosity and boundary conditions. For this purpose, the Navier–Stokes equations and the first-order sensitivity equations are discretized according to the FEV scheme [46–48] more precisely the $P^1_{NC}\backslash P^0 + P^1$. This numerical scheme is a modification of the Crouzeix–Raviart scheme [49]. The FEV scheme is implemented in the industrial open-source code TrioCFD [50,51], a CFD code developed at CEA (French Alternative Energies and Atomic Energy Commission). It is a massively parallel, object-oriented code implemented in C++, dedicated to various scientific and industrial studies and research applications. TrioCFD focuses on addressing problems in the nuclear energy sector through mathematical and computational modeling.

The Navier–Stokes equations are simulated using TrioCFD, and a specific module is developed for the sensitivity equations.

6.1. Uncertain viscosity

The viscosity is considered as the uncertain parameter, uniformly distributed with $\mu = 0.01$ the mean and a standard deviation of 10% of its mean. The viscosity and its sensitivity are written as follows

$$\tilde{\nu}_0 = \mu - \sigma \text{ and } \tilde{\nu}_1 = 1.$$

The Navier–Stokes equations Eq. (34) and their sensitivity equations Eq. (35) are solved with TrioCFD. The results obtained by the PCM are compared with those obtained using Taylor expansion and those obtained in [44].

In Fig. 1 the horizontal and vertical velocity; the solutions of the Navier–Stokes equations Eq. (34) are presented when reaching the stationary state. In Fig. 2, the sensitivity horizontal and vertical velocity; solutions of the first-order sensitivity Navier–Stokes equations Eq. (35) when the stationary state is reached.

In Fig. 3 and Fig. 4 the means and the standard deviation of the horizontal and vertical velocities are respectively represented, when the viscosity in the uncertain parameter.

The Fig. 5(a) and Fig. 5(b) represent respectively the mean and the standard deviation of the horizontal velocity computed according to the PCM detailed in Section 3.1 and compared to the one computed in [44] and the one calculated using Taylor expansion with uncertain viscosity on the horizontal cross-section $y = 0.5$. In We observed a good agreement between the results obtained in [44], the Taylor expansion method detailed in [41], and the PCM used and presented in this paper.

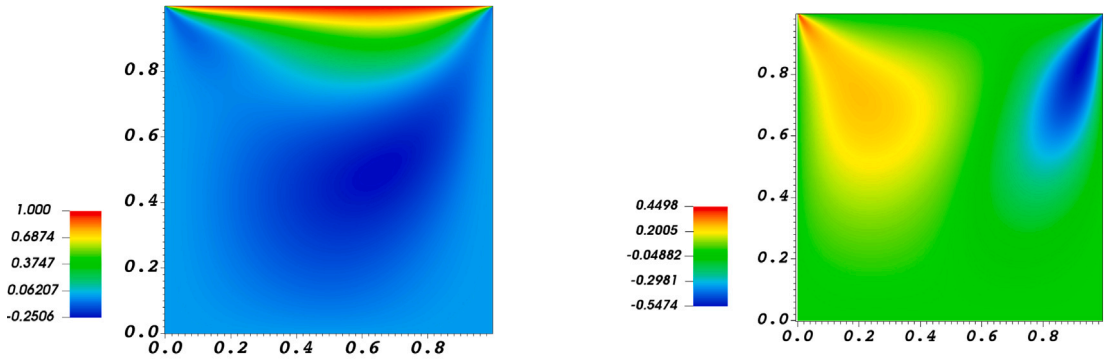

(a) The horizontal velocity (b) The vertical velocity

Fig. 1. The vertical and the horizontal velocity (m/s), solutions of the Navier–Stokes equations.

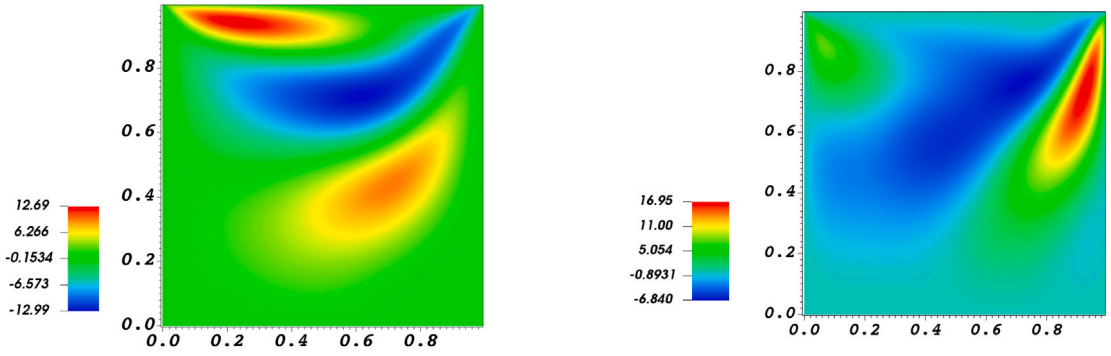

(a) The sensitivity horizontal velocity (b) The sensitivity vertical velocity

Fig. 2. The sensitivity vertical and horizontal velocity (m/s), solutions of the first-order sensitivity of the Navier–Stokes equations.

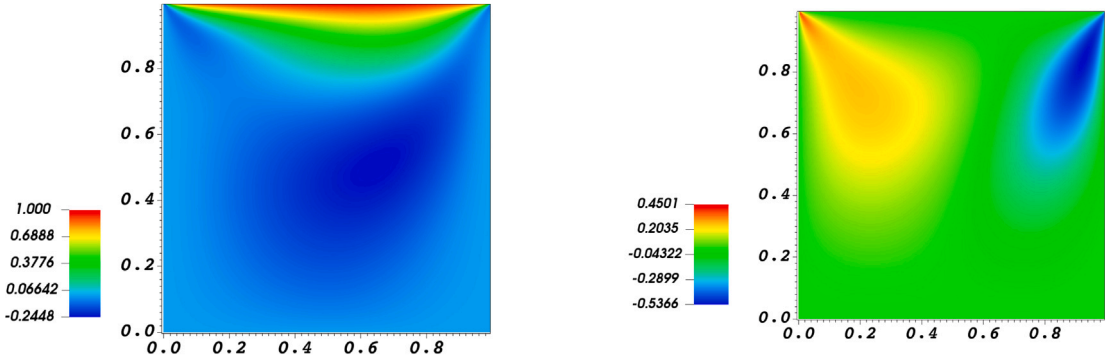

(a) Average of the horizontal velocity (b) Average of the vertical velocity

Fig. 3. A $2d$ presentation of the means of the two components of the velocity u (m/s) and v (m/s), while the viscosity is uncertain.

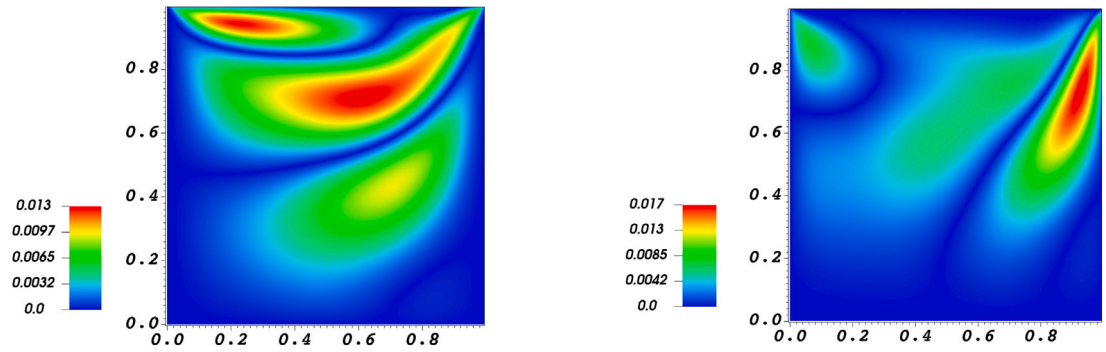

(a) standard deviation of the horizontal velocity

(b) standard deviation of the vertical velocity

Fig. 4. A $2d$ presentation of the standard deviation of the two components of the velocity u (m/s) and v (m/s) while the viscosity is uncertain.

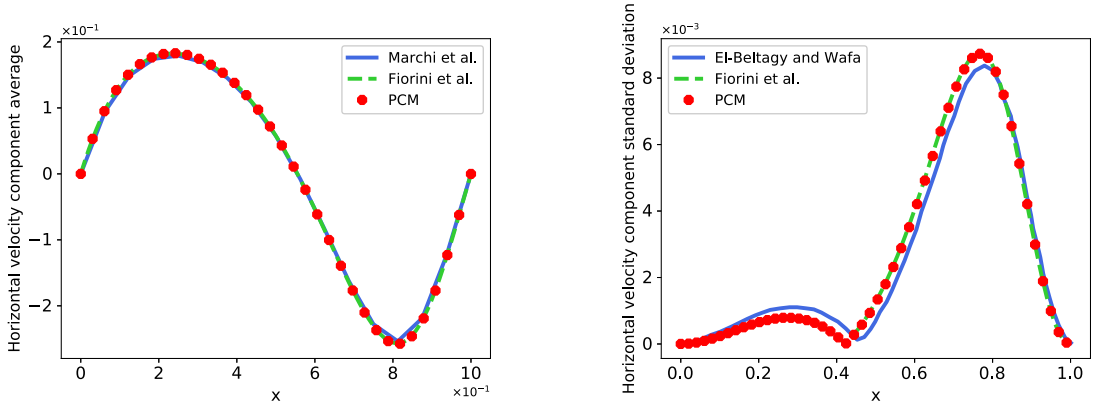

(a) Mean of the horizontal velocity on the horizontal cross-section $y = 0.5$ for random viscosity.

(b) Standard deviation of the horizontal velocity on the horizontal cross-section $y = 0.5$ for random viscosity.

Fig. 5. Comparison of the mean and standard deviation of the horizontal velocity calculated by PCM and Taylor expansion. (a) Mean of the horizontal velocity (m/s). (b) Standard deviation of the horizontal velocity (m/s).

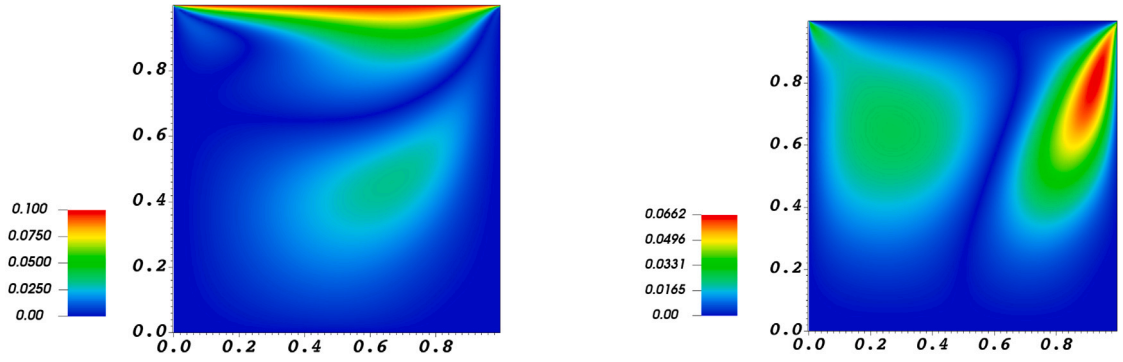

(a) standard deviation of the horizontal velocity

(b) standard deviation of the vertical velocity

Fig. 6. A $2d$ presentation of the standard deviations of the two components of the velocity u (m/s) and v (m/s) for uncertain boundary conditions.

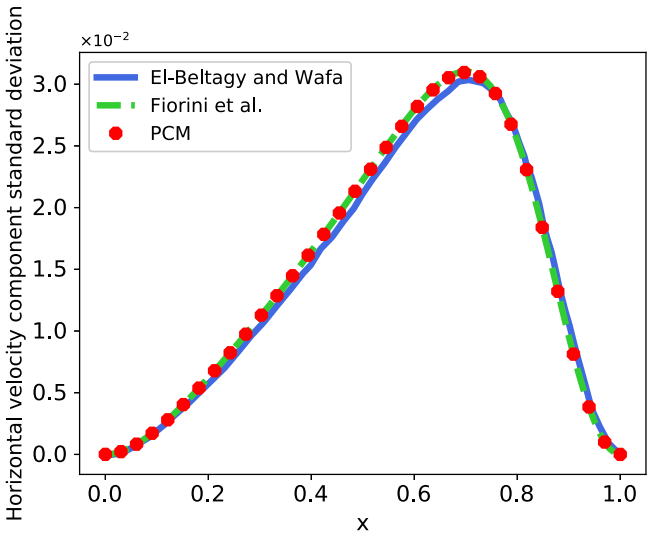

Fig. 7. Comparison between the standard deviation of the horizontal calculated by the PCM and Taylor expansion on the horizontal cross-section $y = 0.5$, for random lid velocity.

6.2. Uncertain boundary condition

In this section, we set the lid-driven velocity as a random variable to investigate the influence of uncertainty of boundary conditions. The mean value of the lid driven velocity μ_v is set to 1 with a standard deviation σ_v of 10% of the mean value. The viscosity coefficient ν is 0.01. In this numerical test, we have an uncertainty boundary condition on the upper wall of the domain. We will perform the same numerical test using the PCM, presented in Section 3.1. Eq. (34) and (35) are solved with uncertain lid-driven velocity. The lid-driven velocity and its sensitivity is written as follows

$\tilde{u}_0 = \mu - \sigma$ and $\tilde{u}_1 = 1$.

The discretization of both the state and the sensitivity equations are developed and solved in TrioCFD. The results obtained by the PCM are compared with those obtained in [44] and the ones obtained using the Taylor expansion method. We observed a good agreement between the standard deviations of the uncertain variables computed in [44], the ones computed according to the Taylor expansion method, and the PCM presented in this paper. In Fig. 6, the standard deviation of the horizontal and vertical velocity when the boundary condition is uncertain. In Fig. 7, the standard deviation of the horizontal velocity computing according to the PCM detailed in Section 3.1 and compared to the one computing in [44] and the one computing using Taylor expansion with uncertain lid velocity on the horizontal cross-section $y = 0.5$.

6.3. Uncertain viscosity and boundary condition

The mixed random variation of both the viscosity and the lid velocity is evaluated. As a result of Eq. (7), the standard deviation of velocity represents the sum of the standard deviation of velocity when the viscosity is uncertain and the standard deviation when the lid velocity is uncertain. In Fig. 8, the standard deviation of the horizontal and vertical velocity when both uncertain viscosity and uncertain boundary conditions together. Comparison between the standard deviation of the horizontal velocity component calculated according to the multivariate PCM detailed in Section 3.2, Taylor expansion, and the results obtained in [44], is shown in Fig. 9. Once again, we observed a good agreement between the three standard deviations computed according to [44], the PCM presented and used in this article and the Taylor expansion method described in [41]. The effect of the uncertainty in the lid-driven velocity and the viscosity together is less than the single variation in lid velocity but more significant than the effect of the uncertain viscosity.

7. Conclusion

This paper presents a comprehensive framework for the efficient representation and propagation of uncertainty in the Navier–Stokes equations using the intrusive PCM, also known as the Stochastic Galerkin method. We consider the case where uncertainties exist in input parameters, specifically in viscosity or initial/boundary conditions. The governing equations are projected onto stochastic basis functions. In this work, we focus on the first-order PCM. After applying this approach to the Navier–Stokes equations, two coupled systems yielded. To facilitate their resolution, we perform a decoupling step, resulting in two decoupled systems: the Navier–Stokes system itself and the first-order sensitivity of the Navier–Stokes equations. The analysis of the well-posedness and stability of the first-order sensitivity Navier–Stokes equations is presented in this paper. It is demonstrated through an energy estimate of the sensitivity velocity. Additionally, the multivariate PCM is considered in this work. This method is particularly efficient for computing an uncertain variable's mean and standard deviation when there is more than one uncertain parameter. The lid-driven cavity numerical test is presented in this paper. Three scenarios are conducted: the first involves uncertain viscosity, the second involves uncertain lid-driven velocity, and the third involves uncertainty in both parameters. In each case, the mean and standard deviation of the vertical and

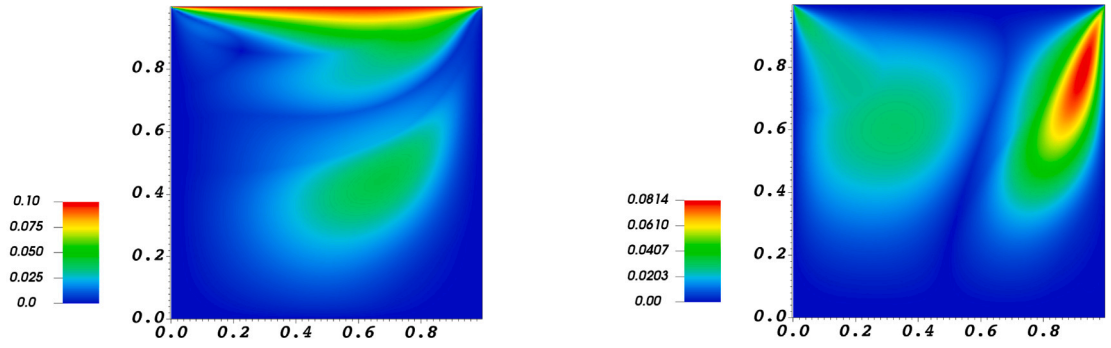

(a) standard deviation of the horizontal velocity

(b) standard deviation of the vertical velocity

Fig. 8. A $2d$ presentation of the standard deviations of the two components of the velocity u (m/s) and v (m/s) for both uncertain viscosity and uncertain boundary condition together.

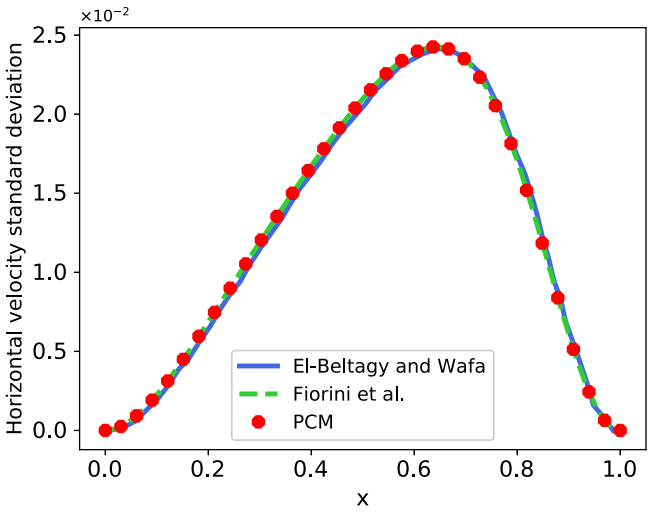

Fig. 9. Comparison between the standard deviation of the horizontal velocity (m/s) calculated by the PCM and Taylor expansion on the horizontal cross-section $y = 0.5$ for both random viscosity and lid velocity.

horizontal velocities are calculated and compared with those from the Taylor expansion method, showing excellent agreement.

As a next step, we intend to adapt the PCM to study the uncertainties in thermohydrodynamics problems and turbulent flows.

CRediT authorship contribution statement

N. Nouaime: Writing – review & editing, Methodology. **B. Després:** Writing – review & editing. **M.A. Puscas:** Writing – review & editing, Software, Methodology. **C. Fiorini:** Writing – review & editing, Methodology.

Declaration of competing interest

The authors declare the following financial interests/personal relationships which may be considered as potential competing interests: Nathalie Nouaime reports financial support was provided by French Alternative Energies and Atomic Energy Commission Saclay Center. Nathalie Nouaime reports a relationship with French Alternative Energies and Atomic Energy Commission Saclay Center that includes: employment. If there are other authors, they declare that they have no known competing financial interests or personal relationships that could have appeared to influence the work reported in this paper.

Data availability

Data will be made available on request.

References

[1] S. Shahane, N.R. Aluru, S.P. Vanka, Uncertainty quantification in three dimensional natural convection using polynomial chaos expansion and deep neural networks, Int. J. Heat Mass Transfer 139 (2019) 613–631.
[2] S. Khatoon, J. Phirani, S.S. Bahga, Fast Bayesian inference for inverse heat conduction problem using polynomial chaos and Karhunen–Loeve expansions, Appl. Therm. Eng. 219 (2023) 119616.
[3] M. De Bastiani, A. Aimetta, R. Bonifetto, S. Dulla, Application of the polynomial chaos expansion to the uncertainty propagation in fault transients in nuclear fusion reactors: DTT TF fast current discharge, Appl. Sci. 14 (3) (2024) 1068.
[4] X. Zhang, S. Dong, W. Dong, Application of polynomial chaos expansion in uncertainty quantification of reactor thermal-hydraulic calculation, in: International Conference on Nuclear Engineering, Vol. 86410, American Society of Mechanical Engineers, 2022, V07AT07A028.
[5] S. Jahanbakhshi, Uncertainty propagation and sensitivity analysis of three-phase flow in porous media using polynomial chaos expansion, J. Nat. Gas Sci. Eng. 103 (2022) 104651.
[6] J. Meng, H. Li, An efficient stochastic approach for flow in porous media via sparse polynomial chaos expansion constructed by feature selection, Adv. Water Resour. 105 (2017) 13–28.
[7] C.P. Rupert, C.T. Miller, An analysis of polynomial chaos approximations for modeling single-fluid-phase flow in porous medium systems, J. Comput. Phys. 226 (2) (2007) 2175–2205.
[8] E. dos Santos Oliveira, U. Nackenhorst, Sparse polynomial chaos expansion for high-dimensional nonlinear damage mechanics, Probabilistic Eng. Mech. 75 (2024) 103556.
[9] D. Xiu, D. Lucor, C.-H. Su, G.E. Karniadakis, Stochastic modeling of flow-structure interactions using generalized polynomial chaos, J. Fluids Eng. 124 (1) (2002) 51–59.
[10] J.A. Witteveen, S. Sarkar, H. Bijl, Modeling physical uncertainties in dynamic stall induced fluid–structure interaction of turbine blades using arbitrary polynomial chaos, Comput. Struct. 85 (11–14) (2007) 866–878.
[11] I.-G. Farcaş, B. Uekermann, T. Neckel, H.-J. Bungartz, Nonintrusive uncertainty analysis of fluid-structure interaction with spatially adaptive sparse grids and polynomial chaos expansion, SIAM J. Sci. Comput. 40 (2) (2018) B457–B482.
[12] H. Dolfen, S. Vandewalle, J. Degroote, Effect of stochastic deformation on the vibration characteristics of a tube bundle in axial flow, Nucl. Eng. Des. 411 (2023) 112412.
[13] P.L.T. Duong, W. Ali, E. Kwok, M. Lee, Uncertainty quantification and global sensitivity analysis of complex chemical process using a generalized polynomial chaos approach, Comput. Chem. Eng. 90 (2016) 23–30.
[14] M. Salloum, P.E. Gharagozloo, Empirical and physics-based mathematical models of uranium hydride decomposition kinetics with quantified uncertainty, Chem. Eng. Sci. 116 (2014) 452–464.
[15] N. Wiener, The homogeneous chaos, Amer. J. Math. 60 (4) (1938) 897–936.
[16] D. Xiu, G.E. Karniadakis, Modeling uncertainty in flow simulations via generalized polynomial chaos, J. Comput. Phys. 187 (1) (2003) 137–167.
[17] J.A. Witteveen, H. Bijl, Modeling arbitrary uncertainties using gram-Schmidt polynomial chaos, in: 44th AIAA Aerospace Sciences Meeting and Exhibit, 2006, p. 896.
[18] P. Bonnaire, P. Pettersson, C. Silva, Intrusive generalized polynomial chaos with asynchronous time integration for the solution of the unsteady Navier–Stokes equations, Comput. Fluids 223 (2021) 104952.
[19] N. Nouaime, B. Després, M. Puscas, C. Fiorini, Stability of a continuous/discrete sensitivity model for the Navier–Stokes equations, Internat. J. Numer. Methods Fluids (2024).
[20] S. Hosder, R. Walters, R. Perez, A non-intrusive polynomial chaos method for uncertainty propagation in CFD simulations, in: 44th AIAA Aerospace Sciences Meeting and Exhibit, 2006, p. 891.
[21] T.A. Mara, W.E. Becker, Polynomial chaos expansion for sensitivity analysis of model output with dependent inputs, Reliab. Eng. Syst. Saf. 214 (2021) 107795.
[22] D. Métivier, M. Vuffray, S. Misra, Efficient polynomial chaos expansion for uncertainty quantification in power systems, Electr. Power Syst. Res. 189 (2020) 106791.
[23] J. Pereira, J.S. e Moura, A. Ervilha, J. Pereira, On the uncertainty quantification of blood flow viscosity models, Chem. Eng. Sci. 101 (2013) 253–265.
[24] S. Sankaran, H.J. Kim, G. Choi, C.A. Taylor, Uncertainty quantification in coronary blood flow simulations: impact of geometry, boundary conditions and blood viscosity, J. Biomech. 49 (12) (2016) 2540–2547.
[25] C.L. Pettit, Uncertainty quantification in aeroelasticity: recent results and research challenges, J. Aircr. 41 (5) (2004) 1217–1229.
[26] M.A. Puscas, R. Lagrange, Interaction of two cylinders immersed in a viscous fluid. On the effect of moderate Keulegan–Carpenter numbers on the fluid forces, Eur. J. Mech. B Fluids 101 (2023) 106–117.
[27] R. Lagrange, M.A. Puscas, Viscous theory for the vibrations of coaxial cylinders: Analytical formulas for the fluid forces and the modal added coefficients, J. Appl. Mech. 90 (6) (2023) 061009.
[28] S.B. Furber, J.E. Ffowcs Williams, Is the Weis-Fogh principle exploitable in turbomachinery? J. Fluid Mech. 94 (1979) 519–540.
[29] C. Eloy, R. Lagrange, C. Souilliez, L. Schouveiler, Aeroelastic instability of cantilevered flexible plates in uniform flow, J. Fluid Mech. 611 (2008) 97–106.
[30] P. Pettersson, J. Nordström, A. Doostan, A well-posed and stable stochastic Galerkin formulation of the incompressible Navier–Stokes equations with random data, J. Comput. Phys. 306 (2016) 92–116.
[31] M. Navarro, J. Witteveen, J. Blom, Polynomial chaos expansion for general multivariate distributions with correlated variables, 2014, arXiv preprint arXiv:1406.5483.
[32] J. Feinberg, V.G. Eck, H.P. Langtangen, Multivariate polynomial chaos expansions with dependent variables, SIAM J. Sci. Comput. 40 (1) (2018) A199–A223.
[33] R. Temam, Navier-Stokes Equations: Theory and Numerical Analysis, vol. 343, American Mathematical Soc., 2001.
[34] V. Girault, P.-A. Raviart, Finite Element Methods for Navier-Stokes Equations: Theory and Algorithms, vol. 5, Springer Science & Business Media, 2012.

[35] H. Bijl, D. Lucor, S. Mishra, C. Schwab, Uncertainty quantification in computational fluid dynamics, in: Lecture Notes in Computational Science and Engineering, Springer International Publishing, 2013.
[36] T. Crestaux, O. Le Maître, J.-M. Martinez, Polynomial chaos expansion for sensitivity analysis, Reliab. Eng. Syst. Saf. 94 (7) (2009) 1161–1172, Special Issue on Sensitivity Analysis.
[37] J.A. Paulson, E.A. Buehler, A. Mesbah, Arbitrary polynomial chaos for uncertainty propagation of correlated random variables in dynamic systems, IFAC-Pap. 50 (1) (2017) 3548–3553.
[38] M. Eldred, C. Webster, P. Constantine, Evaluation of non-intrusive approaches for Wiener-Askey generalized polynomial chaos, in: 49th AIAA/ASME/ASCE/AHS/ASC Structures, Structural Dynamics, and Materials Conference, 16th AIAA/ASME/AHS Adaptive Structures Conference, 10th AIAA Non-Deterministic Approaches Conference, 9th AIAA Gossamer Spacecraft Forum, 4th AIAA Multidisciplinary Design Optimization Specialists Conference, 2008, p. 1892.
[39] D. Gottlieb, D. Xiu, Galerkin method for wave equations with uncertain coefficients, Commun. Comput. Phys. 3 (2) (2008) 505–518.
[40] D. Xiu, J. Shen, Efficient stochastic Galerkin methods for random diffusion equations, J. Comput. Phys. 228 (2) (2009) 266–281.
[41] C. Fiorini, B. Després, M.A. Puscas, Sensitivity equation method for the Navier-Stokes equations applied to uncertainty propagation, Internat. J. Numer. Methods Fluids 93 (1) (2021) 71–92.
[42] O. Le Maître, O.M. Knio, Spectral Methods for Uncertainty Quantification: With Applications to Computational Fluid Dynamics, Springer Science & Business Media, 2010.
[43] O.P. Le Maître, O.M. Knio, H.N. Najm, R.G. Ghanem, A stochastic projection method for fluid flow: I. Basic formulation, J. Comput. Phys. 173 (2) (2001) 481–511.
[44] M.A. El-Beltagy, M.I. Wafa, et al., Stochastic 2D incompressible Navier-Stokes solver using the vorticity-stream function formulation, J. Appl. Math. 2013 (2013).
[45] C. Fiorini, M.A. Puscas, B. Després, Sensitivity analysis for a thermohydrodynamic model: Uncertainty analysis and parameter estimation, Eur. J. Mech. B Fluids 105 (2024) 25–33.
[46] P. Emonot, Méthode de volumes éléments finis : applications aux équations de Navier-Stokes et résultats de convergence (Ph.D. thesis), Université Claude Bernard – Lyon I, 1992.
[47] S. Heib, Nouvelles discrétisations non structurées pour des écoulements de fluides à incompressibilité renforcée (Ph.D. thesis), Université Paris VI, 2003.
[48] T. Fortin, Une méthode éléments finis à décomposition L^2 d'ordre élevé motivée par la simulation d'écoulement diphasique bas Mach (Ph.D. thesis), Université Pierre et Marie Curie – Paris VI, 2006.
[49] R.P.-A. Crouzeix M., Conforming and nonconforming finite element methods for solving the stationary Stokes equations I, ESAIM: Math. Model. Numer. Anal. - Modélisation Mathématique et Anal. Numérique 7 (R3) (1973) 33–75.
[50] P.-E. Angeli, M.-A. Puscas, G. Fauchet, A. Cartalade, FVCA8 benchmark for the Stokes and Navier-Stokes equations with the TrioCFD code – benchmark session, in: Finite Volumes for Complex Applications 8, Lille, France, 2017.
[51] U. Bieder, E. Graffard, Qualification of the CFD code Trio_U for full scale reactor applications, Nucl. Eng. Des. 238 (3) (2008) 671–679.